J. Fluid Mech. (1974), *vol.* 64, *part* 4, *pp.* 679–699
Printed in Great Britain

Use of a pseudo-turbulent signal to calibrate an intermittency measuring circuit

By R. A. ANTONIA AND J. D. ATKINSON
Department of Mechanical Engineering, University of Sydney

(Received 11 October 1973)

Measurements of the intermittency factor γ and in particular the crossing frequency f_γ of the turbulent/non-turbulent interface in the outer regions of various turbulent shear flows depend strongly on the settings of the intermittency meter used. Two methods of calibrating an intermittency meter of conventional design are described. In the first, turbulent and non-turbulent signals are simulated and switched at random times using an analog computer. Particular attention is given to the spectra of the switching and turbulent signals but the non-turbulent signal is assumed to have the same spectrum as the turbulent signal. In the second method, the same switching process is applied to two real signals, obtained in the fully turbulent and irrotational flow regions associated with a turbulent jet with a co-flowing external air stream. A rather simple calibration procedure derived using the results of both methods is applied to the measurements of γ and f_γ in the same jet. It is suggested that the simulation process adopted here could be useful in inferring properties of intermittent turbulent flows.

1. Introduction

The study of the turbulent/non-turbulent interface in both free shear flows and partially bounded flows (such as boundary layers and wall jets) remains of predominant importance in the understanding of the entrainment process and hence the growth rate of these flows. Two of the most obvious quantities that can be measured at a point in the intermittent zones of these flows are γ, the fraction of time for which the flow is turbulent, and f_γ, the frequency of crossing of the interface. If an intermittency function $I(t)$, equal to one when the flow is turbulent at the point of measurement and zero when it is not, can be produced, then γ is the average value of $I(t)$, and f_γ its average frequency. Once the interface passage can be successfully detected, a number of statistical features can be investigated for both the rotational and irrotational parts of the flow. The recent use of conditional sampling techniques in turbulent flows has produced a variety of quantitative measures for these features.

The least subjective way to distinguish between turbulent and irrotational flow is to measure vorticity. As this measurement is rather difficult, most of the intermittency detecting circuits that have been developed rely essentially on comparing a signal such as $\partial u/\partial t$, the time derivative of the streamwise velocity component, with rather arbitrary criteria involving one or more adjustable

parameters. The subjectiveness of the criterion is of little importance in determining γ, the intermittency factor, since repeatable measurements of γ have been obtained by a number of different authors using different methods. The distribution of f_γ (see §2), however, shows order-of-magnitude discrepancies, due no doubt to the rather greater accuracy required of $I(t)$ in this case. There is little doubt that inaccuracy in $I(t)$ similarly affects a number of the measured conditional averages to be found in the literature (e.g. Kovasznay, Kibens & Blackwelder 1970; Wygnanski & Fielder 1970; Antonia 1972; Hedley & Keffer 1974*a*).

This paper describes an attempt to calibrate an intermittency meter of conventional design (described in §3) with a pseudo-turbulent (intermittent) signal generated using an analog computer. The pseudo-turbulent signal is generated by switching (at random) between two signals, representing the turbulent and non-turbulent signals, obtained from a random signal generator (see §4). The final result is an intermittent signal of known statistical properties and, in particular, of known γ and f_γ, since the intermittency function $I(t)$ is known exactly. A similar calibration procedure was used by Kibens & Kovasznay (1970), but the present method of generating the calibration signal pays more attention to the spectral density of the signal and also to the characteristics of the switching (Kibens & Kovasznay used simple periodic switching).

A more realistic signal for calibrating the intermittency meter can be obtained by randomly switching between a fully turbulent and non-turbulent signal. Rather than attempting to generate these signals on the analog computer it was found more convenient to use two real signals measured simultaneously at the centre-line of a jet and in the irrotational flow region just outside the jet. The calibration of the meter using this procedure was applied to measure γ and f_γ in the intermittent region of the jet.

The results of the calibration are given in §5 in terms of γ and f_γ only, but there are no reasons why more complex quantities such as weighted higher-order moments of the turbulent and non-turbulent quantities should not be included in the calibration procedure.

2. Detection of interface: published results

A number of investigators have measured γ and sometimes f_γ in a number of flows, by either analog techniques (e.g. Townsend 1949; Corrsin & Kistler 1955; Bradbury 1965; Kovasznay *et al.* 1970; Kuo & Corrsin 1971), or using a digital computer (e.g. Kaplan & Laufer 1968; Antonia & Bradshaw 1971). Irrespective of the technique used, the formation of γ relies essentially on the setting of two parameters: C, the threshold, and τ_H, the hold time (in the notation of Kovasznay *et al.*) over which comparison with C is made. Although C and τ_H are usually set somewhat arbitrarily (often as a result of a subjective comparison of the criterion function $e(t)$ chosen and the intermittency function $I(t)$, viewed on an oscilloscope), a reasonable choice for either or both of these values can be made, as discussed by Kovasznay *et al.* (1970) and Hedley & Keffer (1974*b*). The choices of C and τ_H depend of course on the choice of $e(t)$ and are hence determined to a large extent by the spectral characteristics and other statistical properties of the turbulent

and non-turbulent parts of $e(t)$. The function $e(t)$ is usually chosen so as to enhance the turbulent component in relation to the non-turbulent part. The forms for $e(t)$ used by various investigators have been discussed and summarized by Hedley & Keffer (1974*b*) and Bradshaw & Murlis (1973).

There is no doubt that the use of any hold time at all, unless it is of smaller order than the Kolmogorov time scale, i.e. the convection time of the smallest eddies, will lead to the smoothing out of some significant fluctuations in the turbulent/non-turbulent interface. On the other hand, any function $e(t)$, no matter how sophisticated, will contain some spurious indications ('drop-outs' or 'holes'), which will usually be of short duration and can be eliminated by using a long enough hold time. This will be true whether the criterion function is based on signals representing velocities or signals representing scalar quantities convected with the flow, such as smoke or temperature. Bradshaw & Murlis (1973) correctly point out the danger of eliminating the 'drop-outs' as some of these may be genuinely attributable to the sharply re-entrant interface as revealed by smoke photographs whilst others may be a result of the intermittency associated with the dissipation field (of either velocity or scalar fluctuations). Clearly there will be an optimum hold time, which will give the 'right' values of γ and f_γ, and will also lead to an intermittency function which has a high correlation with the 'real' intermittency. One would expect that the better the criterion function, the shorter the optimum hold time; however, it is unlikely that for any criterion function so far proposed this optimum is as short as the Kolmogorov time scale. Visual observation, whether of hot-wire traces or of smoke pictures, also involves a hold time, which varies from case to case as the observer uses his judgement. Although this use of judgement will usually tend to improve the results compared with an instrument using the same criterion function, the fact that it is not a well-defined process leads to some degree of undesirable subjectivity. Of course, in many cases visual observation is either inconvenient or out of the question, so that the choice is between an instrument calibrated using a turbulent signal whose intermittency properties have been established as well as possible by careful observation by several different observers, using an indicator such as temperature or smoke which defines the turbulent/non-turbulent interface fairly clearly; or else one calibrated using a signal whose intermittency properties are artificially generated, and are thus exactly known. Bradshaw & Murlis (1973) recommend that the first choice be adopted with τ_H made as small as possible or completely removed. The latter choice has been made in this work. While it is obviously impossible to simulate exactly all the properties of real turbulence (since most of them have never been measured), it is felt that this deficiency is more than balanced by the increase in objectivity and reproducibility achieved in the calibration. Whether the instrument, however calibrated, is in fact registering the 'real' turbulent/non-turbulent interface cannot be decided conclusively so long as an exact definition of 'turbulence' is not agreed on. This is a different problem, and is not discussed in detail here.

The results for γ and f_γ available in the literature have been obtained with τ_H invariably set to a constant value whilst C, although sometimes also held constant, was usually allowed to vary as the intermittent part of the flow was

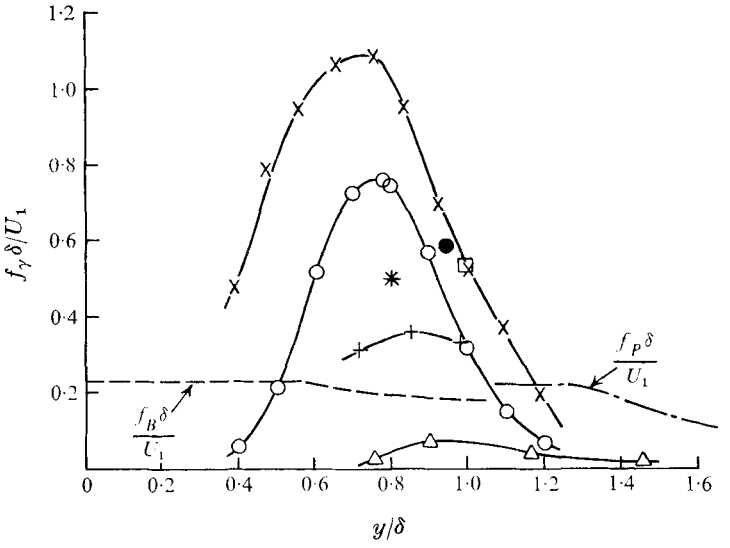

FIGURE 1. Interface crossing and burst frequencies in a boundary layer. Results for f_γ: ○, Kovasznay *et al.* (1970), $R_\theta = 2970$; +, Corrsin & Kistler (1955), $R_\theta = 3800$; ×, Hedley & Keffer (1974*a*), $R_\theta = 9700$; ●, Antonia (1972), $R_\theta = 2140$; □, Antonia (1972), $R_\theta = 4000$; △, Sherman (1972), $R_\theta = 1000$; *, Klebanoff (1955), $R_\theta = 7800$. ——, burst frequency f_B of Narahari Rao *et al.* (1971), $R_\theta = 6550$; — · —, frequency f_P of peak in spectra of u or v, Dumas (1964), $R_\theta = 2900$.

surveyed. Results for γ are well documented in the literature and will not be reproduced here. The variation of γ across the intermittent flow region is found to be closely approximated by the error function

$$\gamma(y) = \tfrac{1}{2}\{1 - \mathrm{erf}[(y-\overline{\eta})/(2\sigma)^{\frac{1}{2}}]\},$$

where y is the distance measured from the wall (in the case of the boundary layer) or from the plane or axis of symmetry (in the case of two-dimensional or axisymmetric jets and wakes), and $\overline{\eta}$ and σ are the mean position and standard deviation respectively of the interface. For nominally self-preserving boundary layers, however, it has been observed that γ is not a universal function of y/δ (δ is the 99·5% boundary-layer thickness), especially for $y/\delta < 1$. Also, small variations are observed in the reported values of $\overline{\eta}/\delta$ and, to a lesser extent, in those of σ/δ for investigations in nominally self-preserving boundary layers with nominally zero-pressure-gradient conditions.† Except perhaps at the lowest Reynolds numbers ($R_\theta < 1000$ say, where $R_\theta = U_1\theta/\nu$, θ being the momentum thickness), it is unlikely that these variations are due to the different Reynolds numbers. They are more likely to be due to the slightly different forms of $e(t)$ used and to the difficulty (cf. Kibens & Kovasznay 1970 and §5) of knowing when the threshold is set correctly.

Distributions in a boundary layer of f_γ, normalized by δ and the free-stream velocity U_1, are shown in figure 1. The maximum values of f_γ occur at approxi-

† Bradshaw (1966) found that, with self-preserving boundary layers in adverse pressure gradients, σ/δ was just significantly larger for the more strongly retarded boundary layer but $\overline{\eta}/\delta$ remained effectively unchanged.

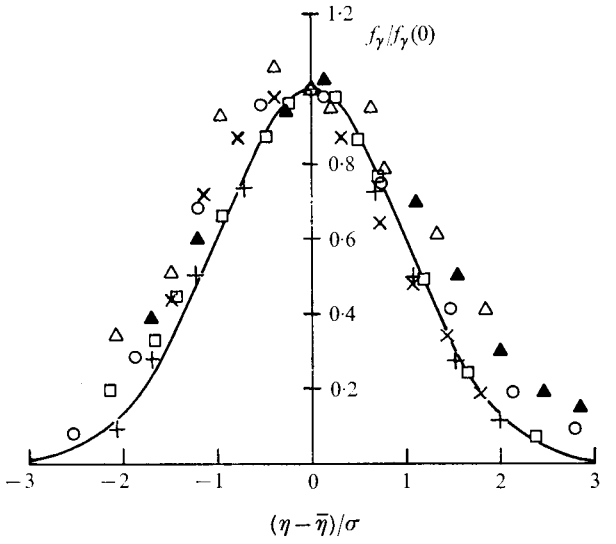

FIGURE 2. Normalized interface frequency results. ×, Hedley & Keffer (1974*a*), boundary layer; ○, Kovasznay *et al.* (1970), boundary layer; △, Wygnanski & Fiedler (1970), high velocity side of mixing layer; ▲, Wygnanski & Fielder (1970), low velocity side of mixing layer; □, present results for round jet; +, Demetriades (1968), wake; ——, Gaussian distribution.

mately the same y/δ position but differ by an order of magnitude, although all the measurements, except those of Corrsin & Kistler (1955)†, were made in a smooth-wall zero-pressure-gradient boundary layer. Sherman's (1972) measurements were made downstream of natural transition in a water boundary layer which developed on the floor of an open channel. Sherman has suggested that the low Reynolds number ($R_\theta = 1000$) and the close proximity to natural transition may account for the extremely low values of f_γ. The other results in figure 1 for f_γ do not show a systematic variation with R_θ. A more plausible explanation for the scatter in the data is the observation (§6) that f_γ is extremely sensitive to the setting of τ_H whereas γ is almost unaffected by τ_H. Also shown for interest in figure 1 are the 'burst' frequencies f_B determined throughout the boundary layer by Narahari Rao, Narasimha & Badri Narayanan (1971) from the analysis of band-passed hot-wire signals, and the peak frequencies f_P deduced from the spectra of u and v (normal) velocity fluctuations obtained by Dumas (1964) in the irrotational part of the boundary layer for $y/\delta > 1{\cdot}1$. The frequencies f_B of Narahari Rao *et al.* (1971) do not vary significantly across the boundary layer and are in close agreement with the boundary-layer measurements of Lu & Willmarth (1972), who define their 'bursts' as contributions to the instantaneous fluctuating Reynolds stress $-uv$ with $u < 0$ and $v > 0$ at a certain threshold level for which the contributions from the other quadrants of the u, v plane are negligible.

† Corrsin & Kistler's measurements were made over a relatively small amplitude wavy wall. Apart from the slightly higher turbulence levels, the characteristics of their boundary layer were essentially the same as those of a smooth-wall layer.

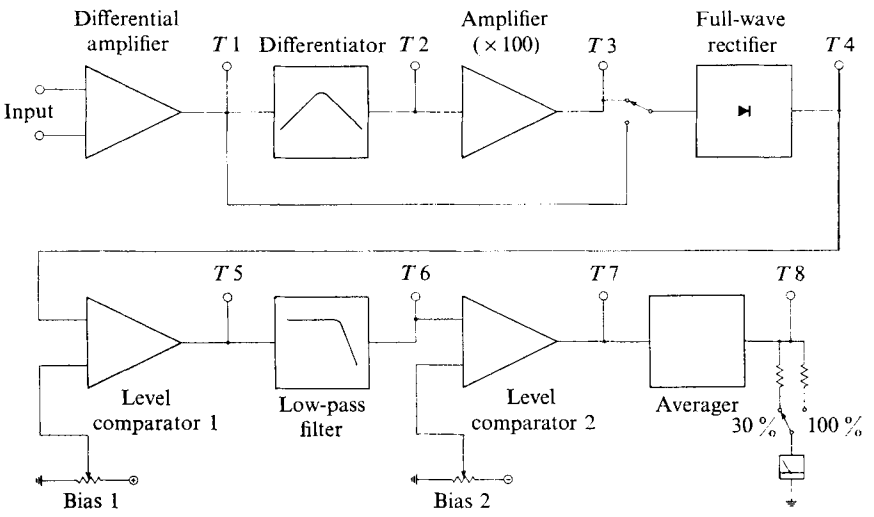

FIGURE 3. Block diagram of intermittency measuring circuit.

However, when the results for f_γ are normalized by $f_\gamma(0)$, the value of f_γ at $y = \overline{\eta}$ (where $\gamma = 0{\cdot}5$ if $\gamma(y)$ is of error-function form), the distributions of figure 1 appear to collapse reasonably closely onto the Gaussian curve

$$\exp\{-\tfrac{1}{2}[(y-\overline{\eta})/\sigma]^2\},$$

as shown in figure 2. In addition to the results of Wygnanski & Fiedler (1970, low and high velocity sides of a mixing layer) the present results for a round jet with a low velocity co-flowing external stream and those of Demetriades (1968) for the supersonic wake of a sphere lie close to the normal curve. Hedley & Keffer (1974*a*) have speculated that the negative skewness of their f_γ distribution and that of Kovasznay *et al.* (1970) may be a result of the folding over the interface. Thomas (1973) also obtains a negatively skewed distribution for f_γ in a two-dimensional wake. In view of the present uncertainty in the measurement of f_γ, especially at low or high values of γ, it may, however, be somewhat premature to comment on the shape of f_γ.

3. Description of intermittency meter

Although the majority of conditionally sampled measurements can be easily obtained only with the use of digital techniques (see Bradshaw 1972), it was both convenient and economical for the present work to use analog techniques. The design of the analog intermittency meter built for this investigation is essentially the same as that used by Townsend (1949), Corrsin & Kistler (1955) and Kuo & Corrsin (1971).

A block diagram of the various processes involved in the intermittency meter is given in figure 3. The input $e(t)$ is first differentiated, then rectified and compared with a variable threshold level C. The differentiator has a frequency response with roll-off of 6 db/octave on either side of the centre frequency of 20 kHz.

The result of the comparison with C is available at the terminal $T5$ (figure 3) and is a random square wave with a number of lapses or holes through a 'turbulent' patch (due to the inevitable zero excursions of the rectified signal) and a number of spurious indications during the 'non-turbulent' part of the signal caused by the signal momentarily exceeding the value of C. To eliminate these spurious indications, the signal is passed through a second-order linear phase low-pass filter. The -3db frequency f_H ($= \tau_H^{-1}$) of this filter was chosen to vary from 4·2 Hz to 202 Hz in logarithmically equal steps. The level of the second comparator was kept fixed at 0·5 times the square-wave amplitude throughout this investigation. The resulting intermittency function $I(t)$ was available at terminal $T7$ whilst γ, the average value of $I(t)$, was displayed on a meter, which was provided with two sensitivities (30% or 100% of full-scale deflexion). A detailed description of the electronics used in the intermittency circuit may be found in Antonia & Stellema (1973).

4. Simulation of intermittently turbulent signal

4.1. *Criteria to be satisfied*

The aim of the simulation was to produce a signal 'resembling' turbulence but with known characteristics, in particular known values of γ and f_γ. The criteria used to ensure that the simulated signal resembled a real signal were as follows.

(i) Its power spectral density should be identical to that of a typical flow variable (to about the same order of accuracy as can be obtained experimentally). The input signal to the intermittency meter was $e(t)$, the fluctuating part of the output voltage of the anemometer, which was directly proportional to the longitudinal velocity $u(t)$. Spectra of $u(t)$ are readily available in the literature for a variety of turbulent shear flows with one or more free stream boundaries.

(ii) Its intermittency characteristics should be identical with those observed for the real signal. Here only a few of the characteristics pertinent to the outer large-scale shear-layer intermittency were reproduced. No attempt was made to incorporate in the fully turbulent part of the signal some of the small-scale intermittency characteristics of turbulence. These characteristics are associated with the intermittent nature of the dissipation process and have been observed by Sandborn (1959) and Narahari Rao *et al.* (1971) in laboratory boundary layers and Frenkiel & Klebanoff (1971) and Kuo & Corrsin (1971) in grid turbulence over a range of turbulence Reynolds numbers. The characteristics of the switching signal that switches between the 'turbulent' and non-turbulent' components should also be as observed in real flows.

(iii) It should be indistinguishable from a real signal when viewed on an oscilloscope. This is the most difficult criterion to satisfy. The difficulties in satisfying it are to some extent tied up with the errors committed in satisfying the two previous criteria. The main difficulty however, is the fact that the real process is not two independent stationary processes with instantaneous independent switching. The real process is continuous, and its average varies throughout the switching cycle.

Two kinds of intermittent pseudo-turbulent signals were used in this study.

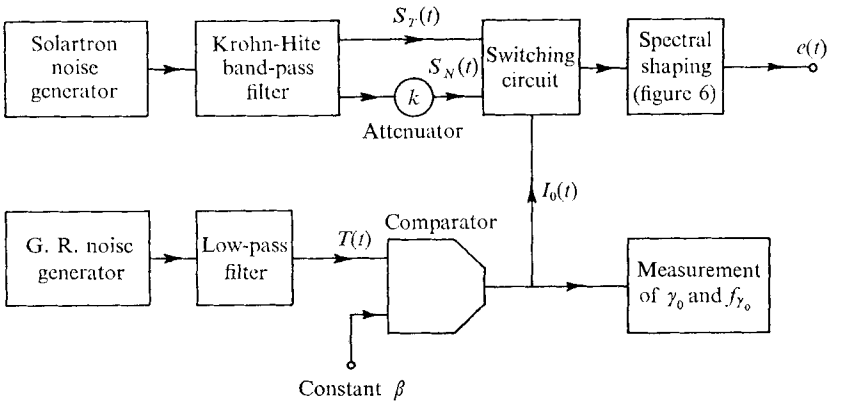

FIGURE 4. Block diagram of circuit for producing the pseudo-intermittent signal.

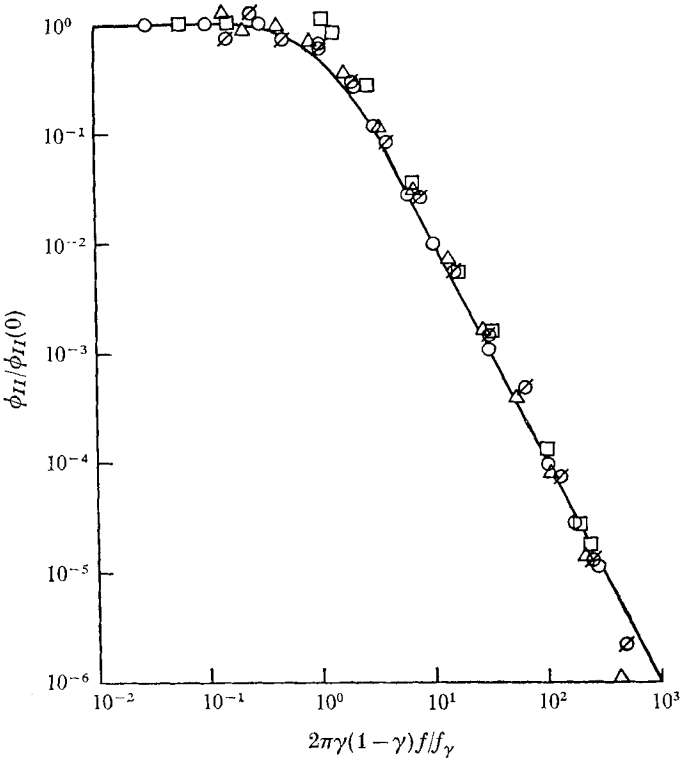

FIGURE 5. Spectra of intermittency functions $I(t)$ and $I_0(t)$. Simulation ($I_0(t)$): ∅, $\gamma_0 = 0{\cdot}51$, $f_{\gamma_0} = 25{\cdot}7$ Hz; △, $\gamma_0 = 0{\cdot}76$, $f_{\gamma_0} = 21{\cdot}8$ Hz. Measurements in jet ($I(t)$): ○, $\gamma = 0{\cdot}20$, $f_\gamma = 32{\cdot}7$ Hz; □, $\gamma = 0{\cdot}49$, $f_\gamma = 73{\cdot}0$ Hz. —, Poisson-distributed switching.

In both cases, switching between the 'turbulent' and 'non-turbulent' components is done using an artificially generated intermittency function $I_0(t)$ In the first, the whole signal is generated artificially. In the second, $I_0(t)$ is used to switch between anemometer signals taken from turbulent and non-turbulent parts of a real flow.

4.2. *Generation of* $I_0(t)$

The artificial intermittency function $I_0(t)$ was obtained, as shown in figure 4, by passing a white-noise signal from a GR ULF noise generator type 418 A through a second-order low-pass filter with break frequency ν, and comparing the resulting signal $T(t)$ with a constant β, so that $I_0(t) = 1$ or 0 according as $T(t) \gtrless \beta$. Varying β and ν gives various values of γ and f_γ. The analog and logic components used formed part of an EAI-180 Analog/Hybrid computer.

For Poisson-distributed switching times, it can be shown that the spectral density of the intermittency function is given by

$$\frac{\phi_{II}(f)}{\phi_{II}(0)} = \left[1 + \left(\frac{2\pi f}{\lambda + \mu}\right)^2\right]^{-1},$$

where λ^{-1} and μ^{-1} are the average durations of the states 0 and 1 respectively. Hence $\lambda + \mu = f_\gamma/[\gamma(1-\gamma)]$, and so

$$\frac{\phi_{II}(f)}{\phi_{II}(0)} = \left\{1 + \left[2\pi\gamma(1-\gamma)\frac{f}{f_\gamma}\right]^2\right\}^{-1}$$

This result is shown on figure 5, together with some measured spectra of $I_0(t)$, and also experimental results from the outer part of the jet described in §4.4. Agreement is good, except perhaps at very high frequencies. Corrsin & Kistler (1955) and Kovasznay *et al.* (1970) have also both found that their experimental results for $\phi_{II}(f)$ were closely approximated by $(1 + Cf^2)^{-1}$, for suitably chosen C. Corrsin & Kistler argued that the probability density of the duration T of the turbulent regions should, for small durations, behave linearly. However, Hedley & Keffer (1974*b*) have found that T for both turbulent and non-turbulent regions is lognormally distributed except for large T, a result similar to that obtained by Narahari Rao *et al.* (1971) for the time intervals between small-scale bursts throughout a boundary layer.

4.3. *Artificially generated spectra*

For simplicity, in a first attempt to simulate $e(t)$, the turbulent and non-turbulent components were assumed to have identical spectra, differing only in amplitude. A block diagram showing the method used is given in figure 4. A Gaussian white-noise signal $S(t)$ from a Solartron Random Signal Generator BO 1227 (spectrum flat from d.c. to 10 kHz, crest factor 6·9: 1) formed both the turbulent signal S_T and, after passing through an attenuator, the non-turbulent signal $S_N\,(= kS_T)$. Switching between the two components was carried out as described above, and the resulting signal filtered linearly to approximate the correct spectrum, using the EAI 180 analog computer.

The spectrum of the streamwise velocity in many turbulent flows can be reasonably approximated by four regions, in each of which it is asymptotic to a

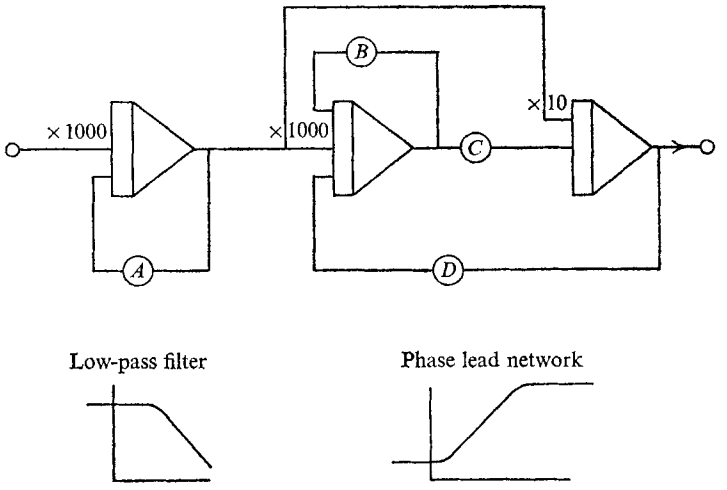

FIGURE 6. Circuit for generating a signal with the spectral density shown in figure 7. *A*, *B*, *C* and *D* are adjustable parameters (attenuators).

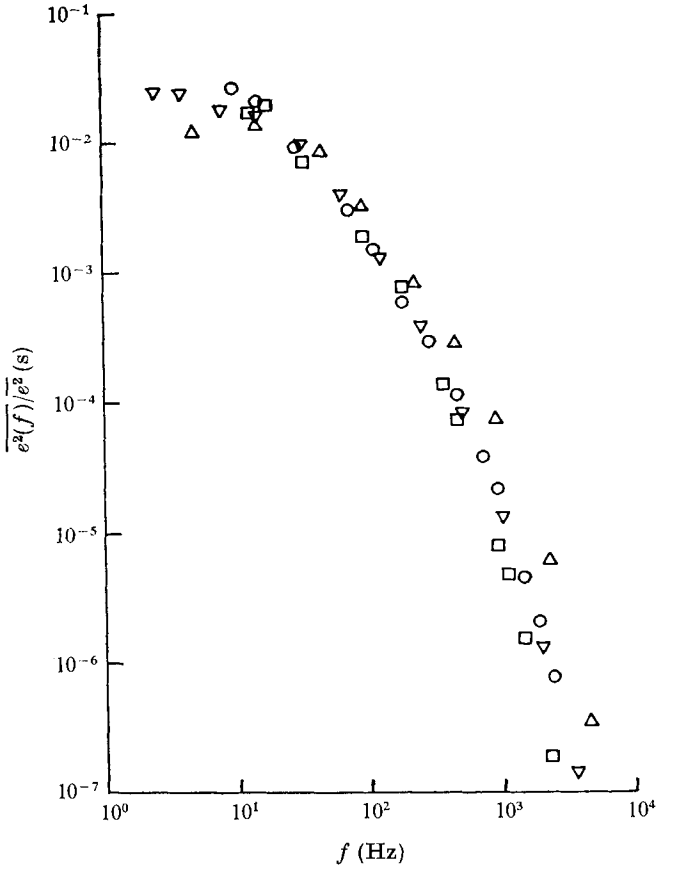

FIGURE 7. Results in jet: △, $y/L_0 = 0$; ○, 1·53; □, 2·08. ▽, simulation on analog computer of ○.

different power of frequency, namely f^0, f^{-1}, $f^{-\frac{5}{3}}$ and f^{-7} (in order of increasing frequency). The same four regions were used in constructing the simulated spectrum, although, because of the linear nature of the filtering, $f^{-\frac{5}{3}}$ and f^{-7} were replaced by f^{-2} and f^{-8} respectively, while the f^{-1} region was replaced by two regions, with f^{-2} and f^0 respectively. The f^{-8} region was obtained using a Krohn–Hite filter model 3750, and the remainder by means of the analog circuit shown in figure 6. (For more details, see Atkinson 1972.) It was found that this method gave spectra which agreed with experimentally found spectra (see figure 7) to well within the accuracy of the latter (typically 10%).

This method of forming $e(t)$ has the disadvantage that spectral shaping is done after switching, so that the spectra of the turbulent and non-turbulent parts cannot be made different (as they certainly are in real flows; see figure 11). This disadvantage can be overcome to some extent by doing some filtering before switching, although this makes the synthesis of a given spectrum more complicated. Complete spectral shaping prior to switching would cause physically impossible discontinuities to appear in $e(t)$ at the time of switching.

4.4. *Switching between two real signals*

Spectra of $e(t)$ obtained at three positions in an axisymmetric turbulent jet developing in an external free stream with small velocity U_1 are shown in figure 7. The signal $e(t)$ was measured with a normal wire operated by a DISA 55M01/55M10 constant-temperature anemometer and its spectrum was analysed with a DISA 55D26 signal conditioner. The simulation of the measured spectrum at $y/L_0 = 1{\cdot}53$ (L_0 is the distance from the centre-line at which the velocity difference $U - U_1 = \frac{1}{2}U_0$, U_0 being the difference between the centre-line velocity and U_1) follows quite closely the experimental points except perhaps for frequencies less than 20 Hz. The exit velocity U_j of the jet was 29·4 m s^{-1} and the ratio $U_j/U_1 = 11{\cdot}4$. The measurements reported in this paper were all made at $x/D = 31{\cdot}5$, where x is the distance from the nozzle and D is the nozzle diameter.

5. Calibration results and discussion

5.1. *Switching between two similar artificial spectra*

The input $e(t)$ to the intermittency measuring circuit was the intermittent signal generated by the method outlined in §§4.2 and 4.3. The spectra of the turbulent signal e_t and non-turbulent signal e_n were identical (as given in figure 7) but the 'noise-to-signal ratio' k ($\equiv \sigma_{e_n}/\sigma_{e_t}$) was varied between 0·2 and 0·7. The mean values of e_t and e_n were made equal to zero. This is clearly not the case in the real flow when $e(t) \equiv u(t)$ (the difference $\overline{u}_t - \overline{u}_n$ of the means of 'zone' averages may be positive or negative, depending on whether the shear is negative or positive). However, the actual value of $\overline{u}_t - \overline{u}_n$ should hav eno effect on the settings of the intermittency meter since the signal is differentiated.

Examples of the results obtained are given in figures 8 and 9 in the form f_γ/f_{γ_0} or γ/γ_0 *vs.* $\sigma_{\dot{e}}/C$, where γ_0 and f_{γ_0} are the true values of γ and f_γ respectively and $\sigma_{\dot{e}}$ is the r.m.s. value of $\dot{e}$ ($= de/dt$). The distributions of f_γ/f_{γ_0} and γ/γ_0 are shown

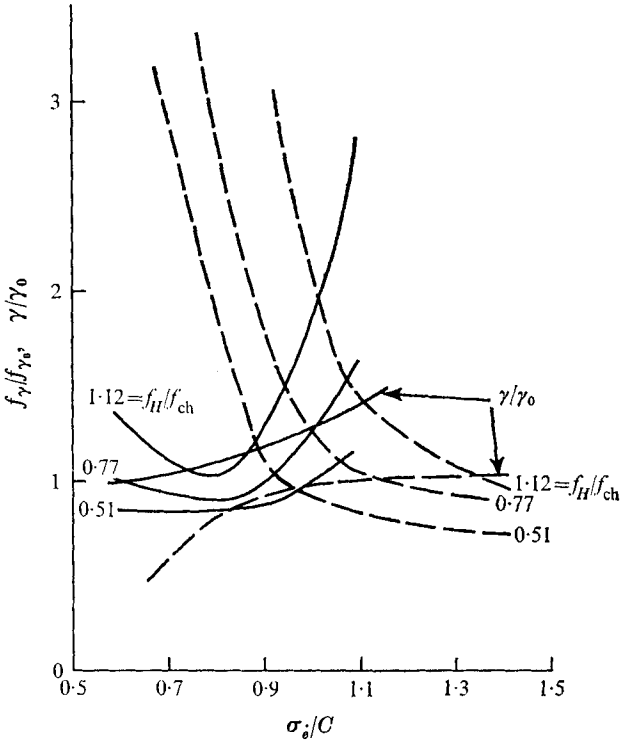

FIGURE 8. Calibration results for switching between two identical simulated spectra ($f_{\gamma_0} = 22\,\text{Hz}, f_{ch} = 180\,\text{Hz}, k = 0{\cdot}3$). ——, $\gamma_0 = 0{\cdot}25$; — —, $\gamma_0 = 0{\cdot}75$.

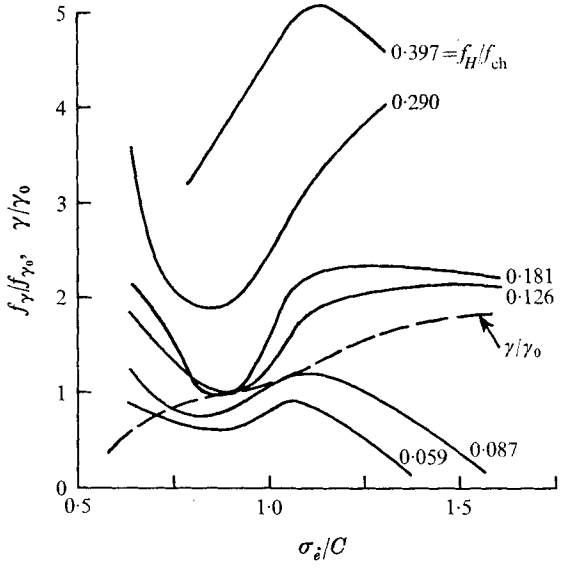

FIGURE 9. Calibration results for switching between two identical simulated spectra for $\gamma_0 = 0{\cdot}50$ ($f_{\gamma_0} = 8{\cdot}3\,\text{Hz}, f_{ch} = 250\,\text{Hz}, k = 0{\cdot}5$). ——, f_γ/f_{γ_0}; — —, γ/γ_0.

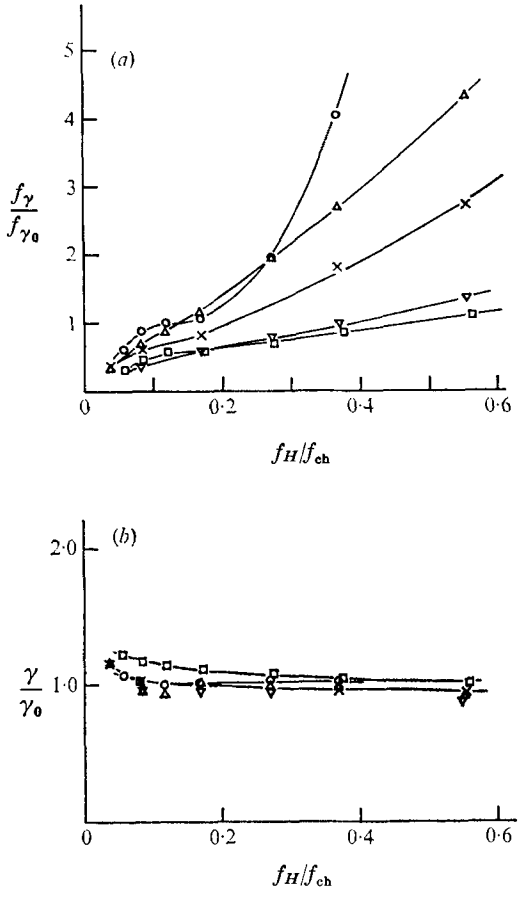

FIGURE 10. Effect of f_H on (*a*) f_γ and (*b*) γ for different values of k and f_{γ_0} ($\gamma_0 = 0.50$, $f_{ch} = 250$ Hz).

	□	○	×	▽	△
k	0·2	0·5	0·5	0·5	0·7
$\sigma_{\dot{e}}/C$	0·93	0·92	0·85	0·89	0·79
f_{γ_0}(Hz)	41	8·3	22	58	23·2

for three values of the filter frequency f_H. This frequency may be normalized by f_{γ_0}/γ_0 or $f_{\gamma_0}/(1-\gamma_0)$, which are inversely proportional to the average durations of a turbulent and non-turbulent occurrence respectively. But since f_{γ_0} and γ_0 are unknown in the real flow, it is more convenient to normalize f_H by the easily measured f_{ch}, a characteristic frequency of the signal defined here by $2\pi f_{ch} = \sigma_{\dot{e}}/\sigma_e$. When $e = u$, f_{ch} is inversely proportional to the Taylor microscale. The selection of the appropriate range of C and f_H for these calibrations was greatly facilitated by displaying simultaneously the traces of e, $\dot{e}$, I_0 and I on a type 549 Tektronix storage oscilloscope.

The results in figure 8 were obtained for $f_\gamma = 22$ Hz and show that, for $\gamma_0 = 0{\cdot}25$, f_γ/f_{γ_0} exhibits a minimum but the position of this minimum clearly does not correspond to the best setting of C, i.e. that setting for which $\gamma = \gamma_0$ and

$f_\gamma = f_{\gamma_0}$.† The distributions γ/γ_0 were only very weakly dependent on f_H over the ranges of f_H considered and are shown in figures 8 and 9 as a single curve. The best value of $\sigma_{\dot{e}}/C$ is almost doubled as γ_0 increases from 0·25 to 0·75 but the optimum value of f_H/f_{ch} is essentially unchanged. The distributions in figure 9 correspond to $k = 0{\cdot}50$, $\gamma_0 = 0{\cdot}50$ and $f_{\gamma_0} = 8{\cdot}3$ Hz ($f_{ch} \simeq 250$ Hz). They also show that f_γ is particularly sensitive to the setting of f_H, the optimum setting for f_H/f_{ch} being near 0·13. Figures 10(*a*) and (*b*) summarize the results obtained with $\gamma_0 \simeq 0{\cdot}50$ over a wide range of f_{γ_0} (8–60 Hz) and k (0·2–0·7). For values of $\sigma_{\dot{e}}/C$ not too different from 0·9 (the optimum setting indicated by the results of figure 9), $\gamma \simeq \gamma_0$ over the whole range of f_H considered here.

The results in figures 8–10 can be compared with those of Kibens & Kovasznay (1970), who also switched between identical spectra but paid less attention to the spectral shape and switching characteristics. One of the main conclusions they drew from their synthetic signal tests was that the best indication of optimum gain is the minimum in the envelope curves as a function of gain. This is not supported by the results of this section. Kibens & Kovasznay also found that f_{γ_0} was overestimated by 15% when $k = 0{\cdot}2$ and by over 50% when $k = 0{\cdot}33$. It would appear that these errors are almost certainly due to f_H being incorrectly set.

5.2. *Switching between two real spectra*

The assumption that the turbulent and non-turbulent spectra are similar is, as shown by the spectra in figure 11, not correct. The spectrum of the non-turbulent signal shown in this figure was measured with the hot wire outside the jet at $y/L_0 = 3{\cdot}0$ and is similar to that of the spectra measured by Dumas (1964) outside a turbulent boundary layer. The 'turbulent' signal was obtained from a second hot wire positioned at $y = 0$ at the same x station. The signals from the two wires were switched by the same circuit (figure 6) as used previously.‡ With $\gamma_0 = 0{\cdot}25$, and a switching frequency $f_{\gamma_0} \simeq 22$ Hz only slightly different from the frequency f_P at which the spectrum of e_n peaks, the spectrum of the switched signal, also shown in figure 11, is similar in shape to the spectra obtained in the intermittent zone of the flow (figure 7). When viewed on the oscilloscope, the switched signal was almost undistinguishable from 'real' signals.

The results of the calibration are given in figure 12 for two values of γ_0. For $\gamma_0 = 0{\cdot}91$, $\gamma \simeq \gamma_0$ over a relatively wide range of $\sigma_{\dot{e}}/C$. The insensitivity of γ to the gain has also been noted by Seshagiri & Bragg (1972) near the centre-line of a cylinder wake where $\gamma \simeq 1{\cdot}0$. Correct values for f_{γ_0} can be obtained for a wide range of f_H but for $\gamma_0 = 0{\cdot}25$, the optimum setting is restricted to

$$f_H/f_{ch} = 0{\cdot}46 \quad (\sigma_{\dot{e}}/C = 0{\cdot}60).$$

† It should be emphasized that, for this setting, I_0 and I, as observed on the storage oscilloscope, are essentially identical apart from the small time delay related to τ_H.

‡ Note that the spectrum of $e_n(t)$ could easily have been synthesized on the analog computer using essentially the procedure outlined in § 4. It was more convenient however to switch between two real spectra. Two of the major difficulties in synthesizing e_t consist of reproducing the small-scale bursting exhibited by fully turbulent signals when they are high-pass or band-pass filtered and also reproducing the slight non-Gaussianity of real signals.

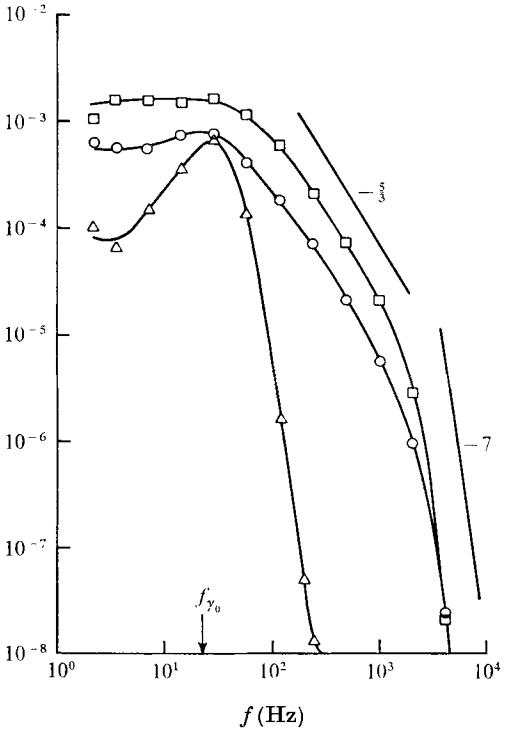

FIGURE 11. Spectra of turbulent and non-turbulent signals for a jet flow: □, e_t spectrum, $y/L_0 = 0$; △, e_n spectrum, $y/L_0 = 3{\cdot}0$; ○, spectrum of simulated signal obtained by switching between e_t and e_n ($\gamma_0 = 0{\cdot}25, f_{\gamma_0} = 22{\cdot}6$ Hz).

Figure 13 summarizes the results obtained for the values of $\sigma_{\dot{\epsilon}}/C$ for which $\gamma \simeq \gamma_0$, over a wide range of γ and f_γ conditions and for three fixed values of f_H. To within the experimental scatter, linear distributions of $\sigma_{\dot{\epsilon}}/C$ *vs.* γ_0 fit the data reasonably well. The results in figure 13 were used to obtain distributions of γ and f_γ (figure 14) in the jet at $x/D = 31{\cdot}5$. The value of f_H was kept fixed and was chosen so that $f_H/f_{\mathrm{ch}} = 0{\cdot}69$ at the first point of measurement ($y/L_0 = 0{\cdot}83$). The procedure used for obtaining γ and f_γ at a given y/L_0 was to (i) pick an initial value of $\sigma_{\dot{\epsilon}}/C$ (a value of 1·0 is a good first guess), (ii) measure γ, (iii) compare γ with the results in figure 13 (in this case, the straight line for $f_H/f_{\mathrm{ch}} = 0{\cdot}69$), (iv) change C and go back to step (ii) if γ does not agree and (v) measure f_γ if the agreement is satisfactory. It was found that only a few iterations were required at each y/L_0 to obtain reasonable agreement with figure 13. Figure 15 shows three distributions of γ and f_γ at the same station in the jet corresponding to three different (but constant) values of C set at $y/L_0 = 0{\cdot}83$, with f_H once more kept constant ($f_H/f_{\mathrm{ch}} = 0{\cdot}69$ at $y/L_0 = 0{\cdot}83$). The γ and f_γ distributions for $\sigma_{\dot{\epsilon}}/C = 1{\cdot}98$ (at $y/L_0 = 0{\cdot}83$) are in close agreement with those of figure 14. This seems to lend some support to the statement, often made in the literature, that a constant setting of C (and also of f_H) can give adequate γ (and f_γ) distributions across the intermittent flow region.

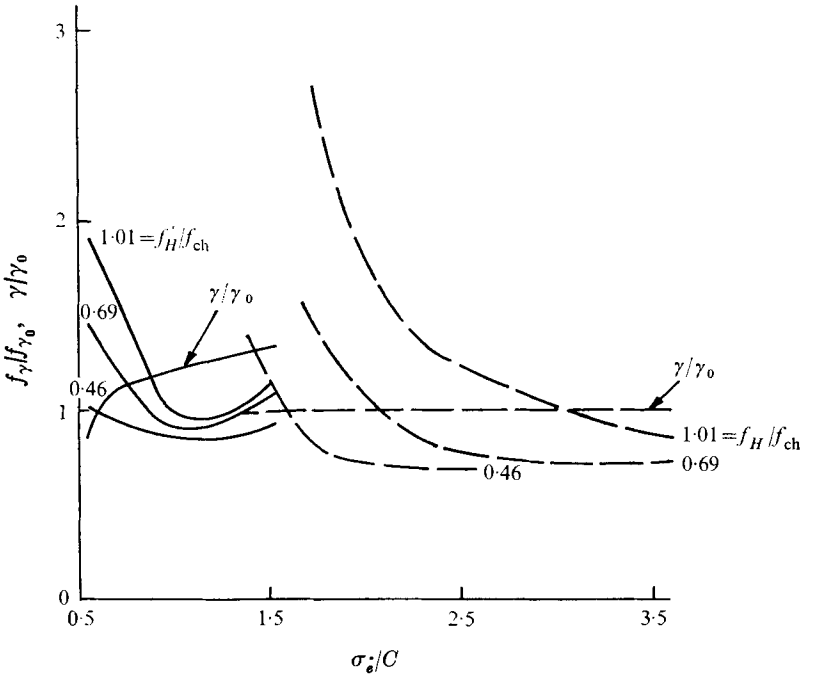

FIGURE 12. Effect of threshold on γ and f_γ, using switching between two real spectra ($f_{ch} = 212$ Hz). ——, $\gamma_0 = 0{\cdot}25$, $f_{\gamma_0} = 23{\cdot}8$ Hz; — —, $\gamma_0 = 0{\cdot}91$, $f_{\gamma_0} = 12{\cdot}3$ Hz.

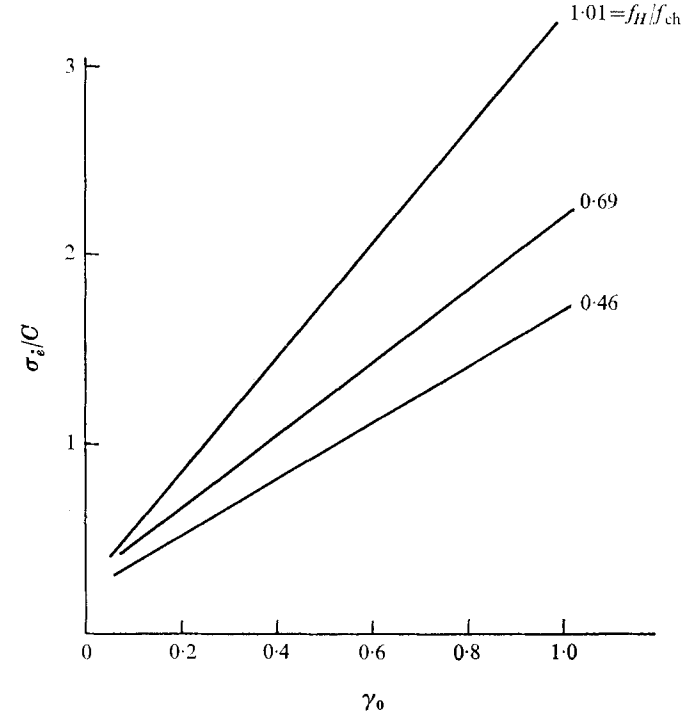

FIGURE 13. Best values of σ_e/C as a function of γ_0 for three values of f_H. Results are for switching between two real spectra ($f_{ch} \simeq 200$ Hz).

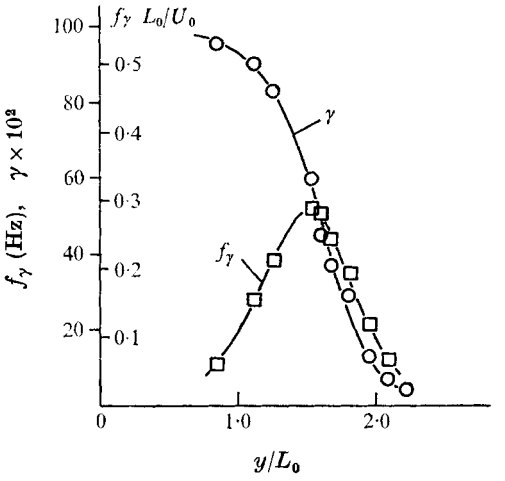

FIGURE 14. Distributions of γ and f_γ across the jet ($x/D = 31{\cdot}5$). The threshold was varied according to results of figure 13 but f_H was kept fixed, corresponding to $f_H/f_{ch} = 0{\cdot}69$ at $y/L_0 = 0{\cdot}83$.

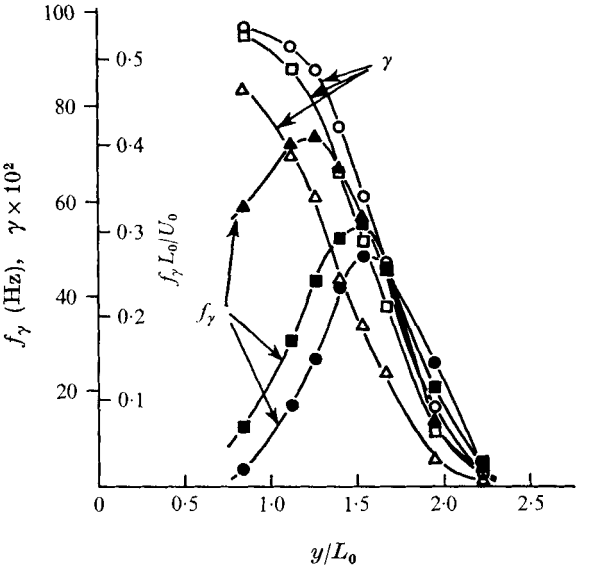

FIGURE 15. Distributions of γ and f_γ across the jet ($x/D = 31{\cdot}5$) for fixed C and f_H. ○, $\sigma_{\dot{\epsilon}}/C = 2{\cdot}94$ and $f_H/f_{ch} = 0{\cdot}69$ at $y/L_0 = 0{\cdot}83$; □, $\sigma_{\dot{\epsilon}}/C = 1{\cdot}98$ and $f_H/f_{ch} = 0{\cdot}69$ at $y/L_0 = 0{\cdot}83$; △, $\sigma_{\dot{\epsilon}}/C = 1{\cdot}21$ and $f_H/f_{ch} = 0{\cdot}69$ at $y/L_0 = 0{\cdot}83$.

6. Recommendations for setting C and f_H

The optimum values of $\sigma_{\dot{\epsilon}}/C$ derived from both the synthetic and real signal tests of § 5 are shown in figure 16. As previously mentioned, these results cover a wide range of k, f_γ and f_{ch}. The straight line corresponding to $f_H/f_{ch} = 0{\cdot}69$ in figure 13 is shown in figure 16 as it was found to give correct values of both γ and f_γ at the lower values of γ. Figure 16 shows that $(\sigma_{\dot{\epsilon}}/C)_{opt} = 2\gamma$ is probably a reasonable fit to the data for calibration purposes.

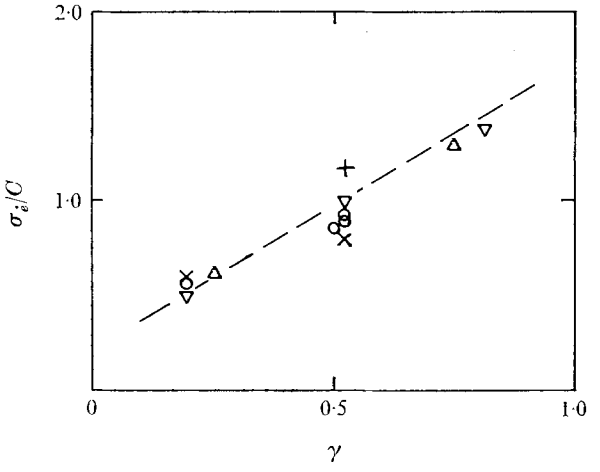

FIGURE 16. Summary of optimum settings of $\sigma_{\dot{e}}/C$ as a function of γ. All symbols refer to switching between pseudo-spectra. +, $k = 0{\cdot}1$; ∇, $k = 0{\cdot}2$; $\triangle$, $k = 0{\cdot}3$; $\bigcirc$, $k = 0{\cdot}5$; $\times$, $k = 0{\cdot}7$.–––, line corresponding to $f_H/f_{ch} = 0{\cdot}69$ in figure 13 and is for switching between real spectra.

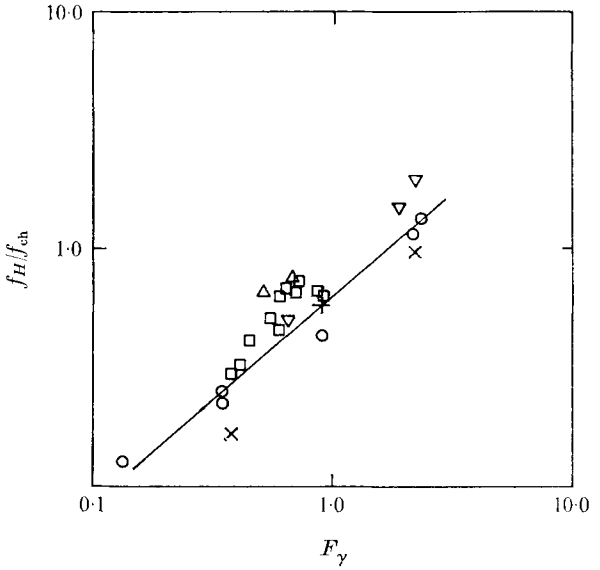

FIGURE 17. Summary of optimum settings of f_H/f_{ch} as a function of F_γ. Symbols for pseudo-spectra are the same as in figure 16. Squares are for real spectra ($k' \simeq 0{\cdot}12$ and $k = 0{\cdot}72$ for all data).

The results in §5 suggest that the optimum setting of f_H/f_{ch} depends on γ, f_γ/f_{ch} and k, although f_γ/f_{ch} is probably the most important. It is reasonable that the hold time should depend on γ only in so far as this influences the average lengths of turbulent bursts (or non-turbulent lapses, if these are shorter). Thus f_H should be a function of f_γ/γ for $\gamma < \frac{1}{2}$, and $f_\gamma/(1-\gamma)$ for $\gamma > \frac{1}{2}$. In order to obtain a single function over the whole range of γ which is smooth at $\gamma = \frac{1}{2}$,

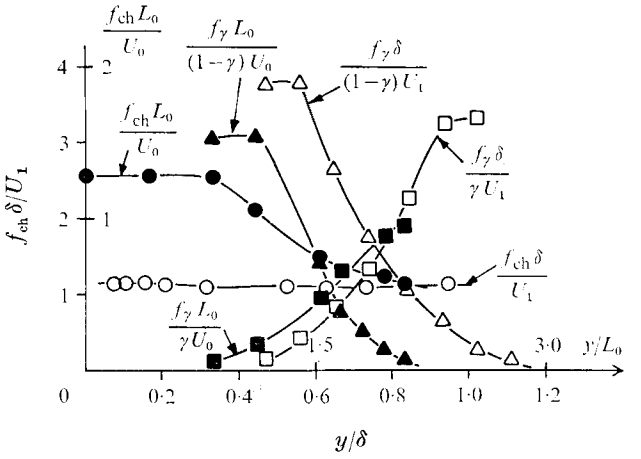

FIGURE 18. Distributions of characteristic frequency f_{ch} and of F_γ in a zero-pressure-gradient boundary layer (data from Kovasznay *et al.* 1970) and in the jet (present results).

f_γ/γ and $f_\gamma/(1-\gamma)$ are replaced by $f_\gamma/\gamma(1-\gamma)$ for all values of γ ($f_\gamma/\gamma(1-\gamma)$ is also the break point in the spectrum of $I(t)$, the intermittency function). In figure 17, optimum values of f_H/f_{ch} are plotted *vs.* $F_\gamma \equiv f_\gamma/\gamma(1-\gamma)f_{ch}$ for all the results available from the two types of calibration tests. The data show considerable scatter (even on a log–log plot!) but seem to suggest a relationship of the form

$$(f_H/f_{ch})_{opt} = b(k)\,F_\gamma^\alpha,$$

where $\alpha = 0{\cdot}8$ and b seems to decrease with increasing k, at least for large values of k. Strictly, the noise-to-signal ratio, k' say, of the differentiated signals should be more relevant than k for correlation purposes. One has $k = k'$ for the synthetic spectra and $k/k' \simeq 6$ for the real spectra, which explains the relative positions of the squares in figure 17.

Although not attempted here, it is relatively easy to allow for the variation of f_H (and also of k or k') in the calibration procedure outlined in § 5.2. The measured values of F_γ in the jet are shown in figure 18 and are in the range 1·4–1·9. The increase in F_γ near the edge of the intermittent region suggests that a constant setting of f_H, as used in figures 14 and 15, is not strictly correct. The f_γ distribution of figure 14 is most likely to be in error for $\gamma > 0{\cdot}5$, where f_H/f_{ch} was set somewhat low. The values of F_γ in a boundary layer (figure 18), inferred from the measurements of Kovasznay *et al.* (1970), are almost twice as high as those in the jet and imply that f_{Hopt} should be certainly larger than f_{ch} in this case. More definite recommendations for setting f_H cannot at present be given, in view of the inconclusiveness of figure 17.

7. Summary of results and final discussion

The calibration of the turbulence intermittency measuring circuit (described in § 3) using a pseudo-turbulent signal derived by random switching between either two signals of similar spectra simulated on an analog computer or two real signals

obtained in the fully turbulent and irrotational regions respectively of a jet has shown the following.

(i) The correct values of γ and f_γ can be obtained over a wide range of γ, f_γ and of the signal-to-noise parameter k provided that both the threshold C and the time constant τ_H of the filter are set correctly.

(ii) C_{opt} depends rather strongly on γ. This dependence is reasonably well defined and seems insensitive to k.

(iii) $\tau_{H\text{opt}}$ depends on γ, f_γ and k. The data are too scattered to enable a definite dependence on these parameters to be postulated but a power-law relationship between f_H and $f_\gamma/\gamma(1-\gamma)$ has been suggested.

The calibration results have been used to obtain satisfactory distributions of γ and f_γ in a round jet. It is hoped that this calibration procedure can be used to obtain more accurate and consistent results for γ and, particularly, f_γ than has hitherto been possible. The accuracy of the calibration method could be improved by paying more attention to the simulation of the pseudo-intermittent signal, in particular to the following points.

(i) The probability density of the turbulent part of the signal is non-Gaussian, the departure from Gaussianity being a function of γ. Although this deviation may be small, it is precisely these small changes which make the prediction of high-order moments of intermittent signals complicated (e.g. Antonia & Atkinson 1973).

(ii) Some allowance should be made for $\overline{u}_t - \overline{u}_n$ and, which will be rather more complicated to realize, for the ensemble average velocities within turbulent and non-turbulent regions. Also, the switching between turbulence and non-turbulence is not independent of the statistics of the turbulent and non-turbulent regions; e.g. large values of $\overline{u}_t - \overline{u}_n$ are in general associated with large durations of turbulent regions whilst $\overline{u}_t \simeq \overline{u}_n$ for small durations.

Besides its use in calibrating instruments such as the intermittent signal, pseudo-turbulence could prove useful in the investigation of theories of turbulence. Even more useful however would be a method which attempted to simulate the basic phenomena occurring in the flow, rather than the statistical properties which are actually measured.

The work described in this paper represents part of a programme of research supported by the Australian Research Grants Committee and the Australian Institute of Nuclear Science and Engineering.

REFERENCES

ANTONIA, R. A. 1972 Conditionally sampled measurements near the outer edge of a turbulent boundary layer. *J. Fluid Mech.* **56**, 1.

ANTONIA, R. A. & ATKINSON, J. D. 1973 High-order moments of Reynolds shear stress fluctuations. *J. Fluid Mech.* **58**, 481.

ANTONIA, R. A. & BRADSHAW, P. 1971 Conditional sampling of turbulent shear flows. *Imp. Coll. Aero. Rep.* no. 71-04.

ANTONIA, R. A. & STELLEMA, L. 1973 Description of an intermittency meter. *Charles Kolling Res. Lab., Dept. Mech. Engng, University of Sydney, Tech. Note*, D-8.

ATKINSON, J. D. 1972 Analog computer simulation of turbulence signals. *Charles Kolling Res. Lab., Dept. Mech. Engng, University of Sydney, Tech. Note*, F-42.

BRADBURY, L. J. S. 1965 The structure of a self-preserving turbulent plane jet. *J. Fluid Mech.* **23**, 31.

BRADSHAW, P. 1966 The turbulence structure of equilibrium boundary layers. *N.P.L. Aero. Rep.* no. 1184.

BRADSHAW, P. 1972 An introduction to conditional sampling of turbulent flows. *Imp. Coll. Aero Rep.* no. 72–18.

BRADSHAW, P. & MURLIS, J. 1973 On the measurement of intermittency in turbulent flow. *Imp. Coll. Aero. Tech. Note*, no. 73–108.

CORRSIN, S. & KISTLER, A. L. 1955 Free-stream boundaries of turbulent flows. *N.A.C.A. Rep.* no. 1244.

DEMETRIADES, A. 1968 Turbulent front structure of an axisymmetric compressible wake. *J. Fluid Mech.* **34**, 465.

DUMAS, R. 1964 Contribution a l'étude des spectres de turbulence. *Publ. Sci. Tech. Min. de l'Air*, no. 404.

FRENKIEL, F. N. & KLEBANOFF, P. S. 1971 Statistical properties of velocity derivatives in a turbulent field. *J. Fluid Mech.* **48**, 183.

HEDLEY, T. B. & KEFFER, J. F. 1974*a* Turbulent/non-turbulent decisions in an intermittent flow. *J. Fluid Mech.* **64**, 625.

HEDLEY, T. B. & KEFFER, J. F. 1974*b* Some turbulent/non-turbulent properties of the outer intermittent region of a boundary layer. *J. Fluid Mech.* **64**, 645.

KAPLAN, R. E. & LAUFER, J. 1968 The intermittently turbulent region of the boundary layer. *Proc. 12th Int. Cong. Appl. Mech.*, p. 236. Springer.

KIBENS, V. & KOVASZNAY, L. S. G. 1970 Detection of the turbulent–non-turbulent interface. *Dept. Mech., The Johns Hopkins University, Rep.* no. 1.

KLEBANOFF, P. S. 1955 Characteristics of turbulence in a boundary layer with zero pressure gradient. *N.A.C.A. Rep.* no. 1247.

KOVASZNAY, L. S. G., KIBENS, V. & BLACKWELDER, R. F. 1970 Large-scale motion in the intermittent region of a turbulent boundary layer. *J. Fluid Mech.* **41**, 283.

KUO, A. Y. S. & CORRSIN, S. 1971 Experiments on internal intermittency and fine-structure distribution functions in fully turbulent fluid. *J. Fluid Mech.* **50**, 285.

LU, S.-S. & WILLMARTH, W. W. 1972 The structure of Reynolds stress in a turbulent boundary layer. *Dept. Aerospace Engng, University of Michigan, Tech. Rep.* no. 021490.

NARAHARI RAO, K., NARASIMHA, R. & BADRI NARAYANAN, M. A. 1971 The bursting phenomenon in a turbulent boundary layer. *J. Fluid Mech.* **48**, 339.

SANDBORN, V. A. 1959 Measurements of intermittency of turbulent motion in a boundary layer. *J. Fluid Mech.* **6**, 221.

SESHAGIRI, B. V. & BRAGG, G. M. 1972 Uncertainty in measurement of intermittency in turbulent free shear flows. *A.I.A.A. J.* **10**, 542.

SHERMAN, D. 1972 Some measurements of the intermittency function in an open channel flow in the region immediately downstream of a natural transition. *Dept. Supply, Aero. Res. Lab. Structures & Materials Note*, no. 374.

THOMAS, R. M. 1973 Conditional sampling and other measurements in a plane turbulent wake. *J. Fluid Mech.* **57**, 549.

TOWNSEND, A. A. 1949 The fully developed turbulent wake of a circular cylinder. *Austr. J. Sci. Res.* A **2**, 451.

WYGNANSKI, I. & FIEDLER, H. E. 1970 The two-dimensional mixing region. *J. Fluid Mech.* **41**, 327.